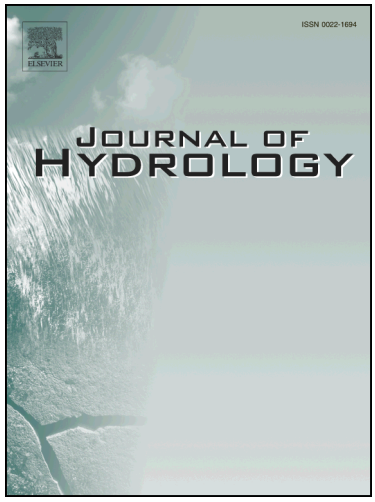

Research papers

How extreme was the October 2015 flood in the Carolinas? An assessment of flood frequency analysis and distribution tails

R.C. Phillips, S.Z. Samadi, M.E. Meadows

PII: S0022-1694(18)30362-7
DOI: https://doi.org/10.1016/j.jhydrol.2018.05.035
Reference: HYDROL 22812

To appear in: *Journal of Hydrology*

Received Date: 27 December 2017
Revised Date: 24 April 2018
Accepted Date: 14 May 2018

Please cite this article as: Phillips, R.C., Samadi, S.Z., Meadows, M.E., How extreme was the October 2015 flood in the Carolinas? An assessment of flood frequency analysis and distribution tails, *Journal of Hydrology* (2018), doi: https://doi.org/10.1016/j.jhydrol.2018.05.035

How extreme was the October 2015 flood in the Carolinas? An assessment of flood frequency analysis and distribution tails

R. C. Phillips[1,2], S. Z. Samadi[1], M. E. Meadows[1]

[1]Department of Civil and Environmental Engineering, University of South Carolina, Columbia, South Carolina USA

[2]Davis & Floyd, Inc., South Carolina, USA

Corresponding author: samadi@cec.sc.edu

Abstract

This paper examines the frequency, distribution tails, and peak-over-threshold (POT) of extreme floods through analysis that centers on the October 2015 flooding in North Carolina (NC) and South Carolina (SC), United States (US). The most striking features of the October 2015 flooding were a short time to peak (T_p) and a multi-hour continuous flood peak which caused intensive and widespread damages to human lives, properties, and infrastructure. The 2015 flooding was produced by a sequence of intense rainfall events which originated from category 4 hurricane Joaquin over a period of four days. Here, the probability distribution and distribution parameters (i.e., location, scale, and shape) of floods were investigated by comparing the upper part of empirical distributions of the annual maximum flood (AMF) and POT with light- to heavy- theoretical tails: Fréchet, Pareto, Gumbel, Weibull, Beta, and Exponential. Specifically, four sets of U.S. Geological Survey (USGS) gauging data from the central Carolinas with record lengths from approximately 65 to 125 years were used. Analysis suggests that heavier-tailed distributions are in better agreement with the POT and somewhat AMF data than more often used exponential (light) tailed probability distributions. Further, the threshold selection and record length affect the heaviness of the tail and fluctuations of the parent distributions. The shape parameter and its evolution in the period of record play a critical and poorly understood role in determining the scaling of flood response to intense rainfall.

Key Words: Flood Frequency Analysis, Return Period, Distribution Tails, The Carolinas.

1. Introduction

The October 3-5, 2015 historic rains caused by hurricane Joaquin released more than 500 mm of rain in South Carolina (SC) and North Carolina (NC), United States (US). The flood peak of many U.S. Geological Survey (USGS) gauges, including those located in the center of SC, were almost twice the previous maximum from a record of over 65 years. The spatial extent of flooding in this portion was also unprecedented, with more record flood peaks at USGS stream gauging stations in urban areas such as Columbia, the capital of SC, than for any other rural catchments.

Such an extraordinary flood lies within the fundamental issue of infrastructure safety and raises the crucial question of how to proceed if this event is not visible for a given dataset and if it is too rare for design applications. Although recently significant progress has been made to predict short-term flood for operational purposes (e.g., Pourreza-Bilondi et al., 2017), long-term prediction, on which infrastructure design is based, is difficult in deterministic terms (e.g., Papalexiou and Koutsoyiannis, 2013). Thus, it is common to treat this event in a probabilistic manner (i.e., as a random variable) that is governed by a distribution law. Such a distribution enables the modeler to capture the probability of exceedance and assign a return period to any flood event, the procedure called flood frequency analysis (FFA) in design hydrology.

Assessment of flood probability has been an active research topic, yet a less understood concept. However, the analysis is well rooted in an extensive literature dating back to the work of Nicolaus Bernoulli three centuries ago (mentioned in Gumbel, 1958). Extreme value theory (EVT) was the first and widely accepted method for FFA that has rapidly evolved and found applications in engineering hydrology. Fuller's 1914 study was probably the first application of extreme value distributions. Some

recent studies, such as Papalexiou and Koutsoyiannis, 2013 and Serinaldi and Kilsby, 2014, 2015, expanded the EVT concepts for hydrological design applications. Specifically, EVT has stimulated an extensive investigation to estimate the parent distribution (e.g., Michele and Rosso, 2001; Bernardara et al., 2008) and (upper) tail behaviors of flood properties (Papalexiou and Koutsoyiannis, 2013; Serinaldi and Kilsby, 2015), just to mention a few recent studies.

Focusing on EVT and referring to Renard et al., 2013 and Martinkova, 2013 for a recent review of the EVT applications in hydrology, this theory captures the asymptotic distributional behavior of two types of data, namely, the so-called block maxima (BM) and peak-over-threshold (POT). BM extracts the maximum values from subsets (i.e., blocks) of observations, whilst POT performs observations exceeding a certain threshold. When the size of the blocks approaches infinity, the distribution of BM converges to three types of extreme value distribution families (Gumbel, Fréchet, and reverse Weibull (Fisher and Tippett, 1928; Gnedenko, 1943)) where the parameters scale with the information dimension. These three types of extreme families can be described by the so-called generalized extreme value (GEV) distribution with the location, scale, and shape parameters (e.g., Coles, 2001) as defined by the unified von Mises-Jenkinson parameterization (Jenkinson, 1955).

If the threshold of exceedance increases, the GEV then converges to the so-called generalized Pareto (GP) distribution as described by the Pickands-Balkema-de Haan theorem (Pickands III, 1975; Balkema and de Haan, 1974). In many cases, GP yields a more accurate approximation to the distribution of absolute and relative excesses, as well as distribution tails. In addition, it represents distribution tails obliquely, but rigorously, by *"letting the data decide the function"*. In practice, a way to verify the validity of GP is to check whether the estimates of the shape parameter are stable when the model is fitted to excesses over a range of thresholds. From a theoretical point of view, absence of the stability can be explained by a slow rate of convergence in the Pickands–Balkema–de Haan theorem. The fitted model can then be used to compute any tail-related risk measure, such as tail probabilities, tail quantiles (or value-at-risk), etc. There

is an established link between GP and GEV in the EVT modeling. In practice, if block maxima follow a GEV distribution, then the threshold excesses have a corresponding approximate distribution within the GP family (e.g., Coles, 2001) and vice versa GEV parameterization can be estimated using GP such as Poisson distribution for the occurrence frequency of the POT (e.g., Goda, 2011).

Recently, the probabilistic fitting of these extreme distributions to hydrological variables signifies major progress in design hydrology as it quantifies risk and disputes arbitrary notions (e.g., Koutsoyiannis, 2004). Although, in spite of the extensive literature on EVA model fitting and goodness-of-fit testing, only few studies have recently tackled the practical problems of flood frequency analysis facing real time application and uncertainty (e.g., Vogel et al., 2011; Stedinger and Griffis, 2011; Rootzén and Katz, 2013; Papalexiou and Koutsoyiannis, 2013; Obeysekera and Salas, 2014; Serinaldi and Kilsby, 2015; Mondal and Mujumdar, 2015). The application of extreme theory on various real-world applications is essential for risk assessment and water resources planning, which demand long time horizons with no other rational scientific basis than probability. Therefore, the aim of this paper is to compute FFA and return periods for annual and instantaneous floods in the center of the Carolinas with special attention to the POT approach and to place the October 2015 flood in a flood frequency analysis context. An important class of questions addressed in this study concerns the impact of peak rates and thresholds on the upper tails of flood distributions. The goal was to investigate the distribution fitting model and the upper- tail distribution of maxima and to provide a better answer to the question of "how extreme was the October 2015 flood in the Carolinas?"

To address aforementioned question, four different applications across the Carolinas were used to infer various procedures and to relate these analyses to properties of the October 2015 flooding. Spatial and temporal variability of flood events and the uncertainty associated with flood properties were also addressed during the period of analysis. The underlying parent distributions were also re-assessed with the inclusion of the 2015 flood event in order to characterize distributional changes associated with the

fitting parameters. This study quantified the sampling uncertainty via confidence intervals (CIs) in the EVT framework to highlight its fundamental role for a fair comparison between models and a fair assessment of the output reliability.

This paper is organized as follows. In Section 2, the study region and flood data used in this study are explained. The theoretical concept and mathematical structures of probability distributions, distribution parameters, and POT are explained in Section 3. These methodologies were then examined in four different case studies explained in Section 4. Each application/example has its own merit, emphasizing particular aspects of extreme analysis. Conclusions are provided in Section 5 as critical guidelines to address the limitation and criticism in judging the magnitude and frequency of floods.

2. Study Area and Data

The study area is located in the eastern US, covering portions of the mountain and piedmont regions of NC and SC. The area is comprised of the Wateree, the Upper and the Lower Broad, the Upper and the Lower Catawba, the South Fork Catawba, the Congaree, the Tyger, the Saluda, and the Enoree sub-basins. Two metropolitan cities, Charlotte and Columbia, are located in the study region (see Figure 1).

Flood data were analyzed to determine appropriate USGS gauges that exhibited a long-term period of record, as well as a consistent hourly/sub-hourly record of the October 2015 flood event. Due to limited data availability and large missing values, this approach limited the analysis to four USGS monitoring gauges. The flood data of USGS 02147500 Rocky Creek at Great Falls, SC, USGS 02160700 Enoree River at Whitmire, SC, USGS 02167000 Saluda River at Chappells, SC, and USGS 02169500 Congaree River at Columbia, SC were used (Figure 1). Historical instantaneous floods data for each of the USGS gauging stations were also collected from October 2, 2015 to October 10, 2015, as well as the period of record data for observed instantaneous flows and peak annual maximum flows.

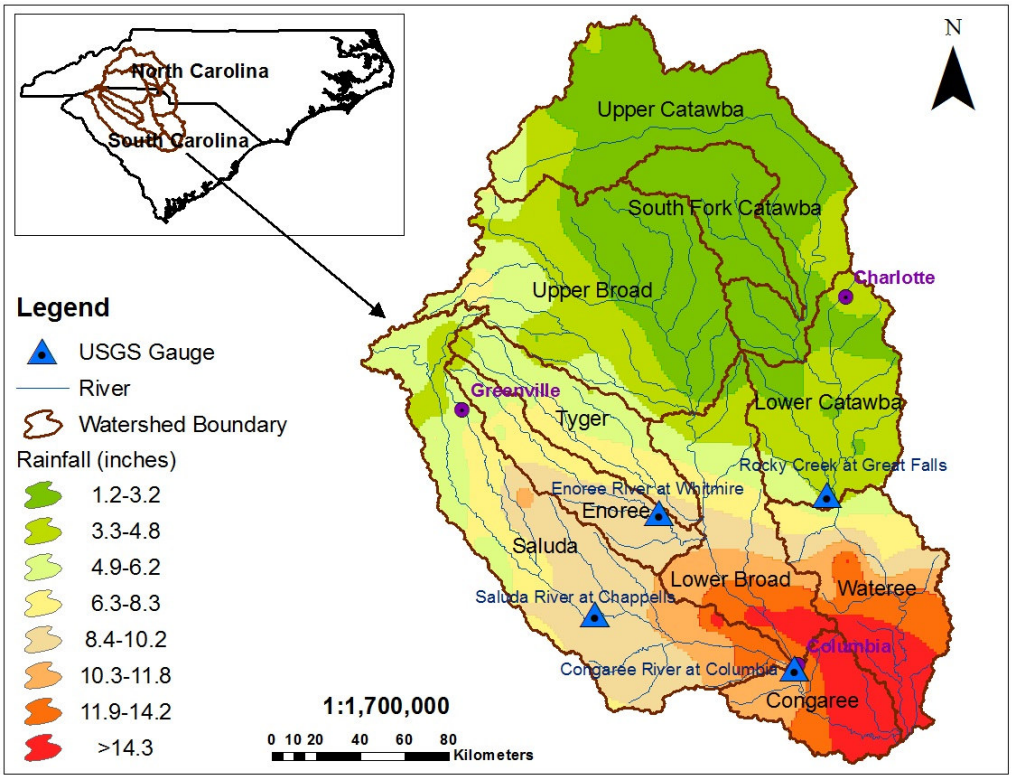

Figure 1. The October 02-05, 2015 total rainfall (inches) in the study area along with four USGS monitoring gages: (i) Rocky Creek at Great Falls, SC, USGS 02147500; (ii) Enoree River at Whitmire, SC, USGS 02160700; (iii) Saluda River at Chappells, SC, USGS 02167000; and (iv) Congaree River at Columbia, SC, USGS 02169500.

Although the rainfall event produced from the hurricane event lasted approximately 3 days, the flood hydrograph spanned for several days as the drainage system responded to intense rainfall for a longer period. Further, the October 2015 intense rainfall produced different runoff volumes, although the time to peak and flood duration are approximately the same among the four hydrographs (Figure 2). It should be noted that all four hydrographs presented in Figure 2 have a short time to peak (T_p) and a continuous peak rate which caused intensive and widespread damages to human lives, properties, and infrastructure. Here, flood data analysis placed emphasis on the concept of "water year," which is often designated as the hydrological year beginning on October 1st and ending on September 30th. Accordingly, two alternative approaches of data are selected: (i) annual maximum flood (AMF) series spanning from 1892 to 2015

with no missing values and (ii) daily maximum flood (DMF) or POT series spanning from October 01, 1984 to September 30, 2015 with less than 3% of missing values.

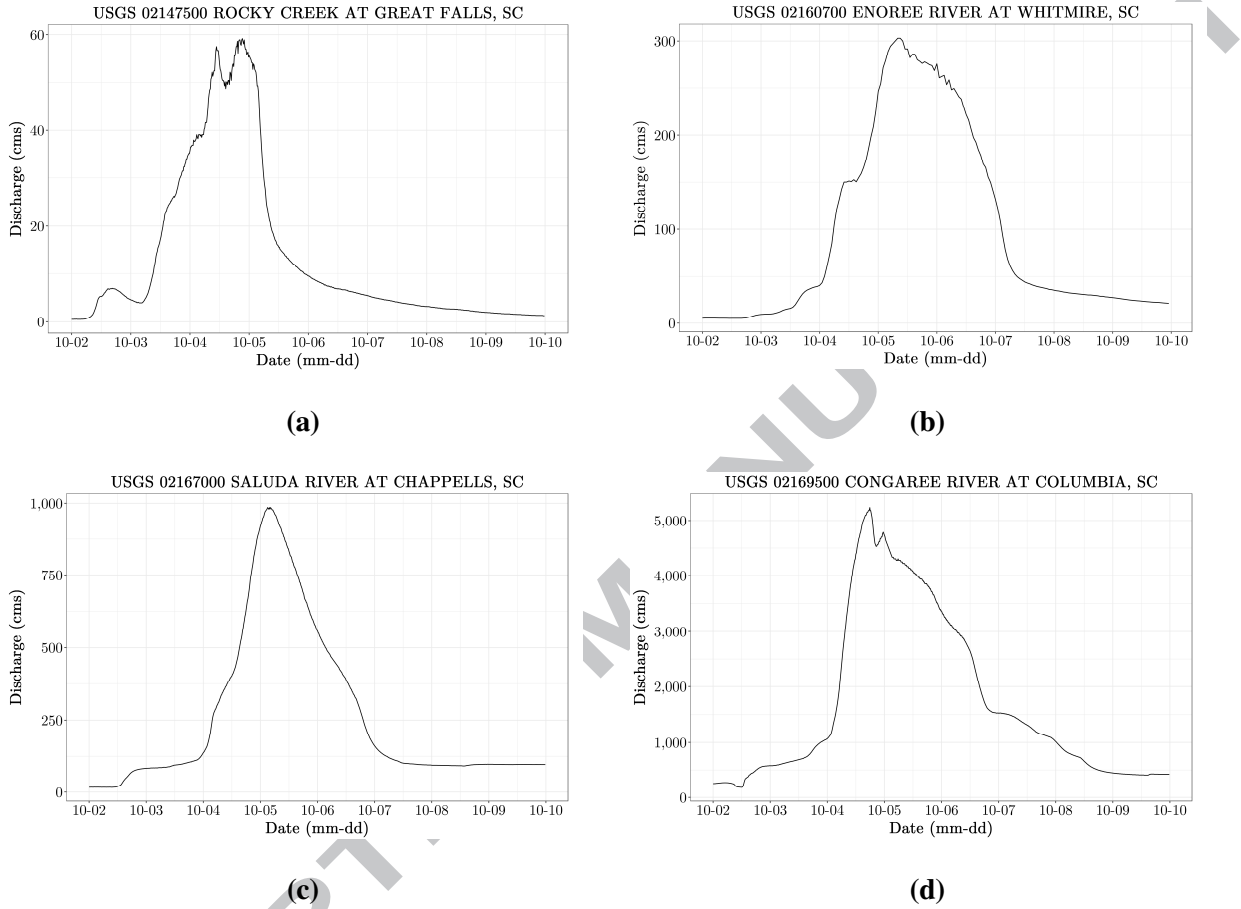

Figure 2. Flood hydrographs resulting from the October 2015 hurricane event for: (a) Rocky Creek; (b) Enoree River; (c) Saluda River; and (d) Congaree River.

3. Methodology

The data sets described in the previous section were employed to fit different distribution functions. This study tested: (i) the significance of lag-1 correlation for two subsequent values by the Kendall correlation coefficient (K-ACF); (ii) possible monotonic trends by the Mann- Kendall (M-K) test; and (iii) distributional hypotheses by goodness of fit and ad hoc diagnostics. Specifically, the suitability of a probability distribution is assessed by four goodness of fit tests, namely, Kolmogorov-Smirnov (K-S),

Cramer-von Mises (C-vM), Anderson-Darling (A-D), and the Pearson product moment correlation coefficient (PPMCC; Kottegoda and Rosso, 2008). K-ACF and M-K tests are necessary to compute the temporal dependence and monotonic trends in data. These trends can also affect the outcome of the goodness of fit tests, which rely on the hypothesis of independent observations (Serinaldi and Kilsby, 2014). In addition to a hypothesis-based goodness-of-fit, information-based criteria (also known as Bayesian statistics) for probability model selection (Laio et al., 2009) was used, which has shown to aid modeler in identifying the best probability distribution for hypothesis testing (e.g., Di Baldassarre et al., 2009; Chen et al., 2017). More specifically, the Akaike Information Criterion (AIC) and Bayes Information Criterion (BIC) were adopted as the information-based criterions. BIC and AIC reward a model for a higher likelihood and penalize a model for overfitting; lower AIC and BIC indicate a better fit. These techniques were implemented using continuous to discrete distributions explained in the next section.

3.1. Theoretical Concept of Probability Distribution

Continuous to more skewed distributions were employed to capture flood characteristics over time. Gumbel is tested as a continuous probability distribution, whereas extreme value theory was used to implement discrete probability distributions. Continuous distributions have been widely applied in hydrology, so we refer the readers to Vogel and Wilson, 1996, Koutsoyiannis, 2005, McMahon et al., 2007, and El Adlouni et al., 2008, among others.

In the classical extreme value theory, if a random variable *(RV) X* follows the distribution $F_X(x)$, the distribution function of the maximum of n is independent and identically distributed (iid) that can be described by

$$G_{Y_n} = F_X(x)^n. \quad (1)$$

If $n \to \infty$, the distribution of n can converge to three limiting laws of the Gumbel, the Fréchet, or the reversed Weibull, which can be described by the unified von Mises-Jenkinson parameterization (Jenkinson, 1955) of the so-called GEV distribution (Coles, 2001)

$$G(z) = \exp\left\{-\left[1+\xi\left(\frac{z-\mu}{\sigma}\right)\right]^{-1/\xi}\right\}, \tag{2}$$

where $\{z: 1+\xi(z-\mu)/\sigma > 0\}$, $\mu \in (-\infty, \infty)\}$ is the location parameter, $\sigma > 0$ is the scale parameter, and $\mu \in (-\infty, \infty)$ is the shape parameter. Depending on the sign of the shape parameter, GEV can envelop three types of distribution functions: i) $\xi > 0$ the heavy-tailed Fréchet; ii) $\xi < 0$ the upper bounded Weibull; and iii) $\xi \to 0$ the Gumbel distribution function.

Based on the Pickands-Balkema-de Haan theorem (Pickands III, 1975; Balkema and de Haan, 1974), a GEV distribution coverages to a GP distribution if the extreme threshold increases over time (Coles, 2001), which is given as

$$H(y) = 1 - \left(1+\xi\frac{y}{\tilde{\sigma}}\right)^{-1/\xi}, \tag{3}$$

where $\{y: y > 0$ and $1+\xi y/\sigma > 0\}$ and $\tilde{\sigma} = \sigma + \xi(u-\mu)$. ξ determines three types of distribution functions (with the same interpretation as for GEV); heavy tail when $\xi > 0$ (i.e., Pareto), upper bound when $\xi < 0$ (i.e., Beta), and exponential in the limit as $\xi \to \infty$. Among three parameters in the EVA theory, ξ plays a key role in hydrological frequency analysis since it determines the upper tail behavior of floods that is important for the design of hydraulic structures.

The point process (PP) model is applied to the distribution of discharge excess following that of the GEV parameterization as outlined by Coles, 2001 and approximated by the GP distribution. PP treats the data points as the occurrence of extreme events and marks their associated size. Briefly, if the parent distribution does not evolve over time (i.e., stationary) and satisfies an asymptotic lack of clustering condition for values that exceed a high threshold, then the distribution's limiting form is non-homogeneous Poisson. It is noted that GEV, PP, GP, and Gumbel distributions were fitted to the AMF data, while only GP and PP models were tested for the POT dataset.

Application of the GP and PP distributions to AMF data is not typically applied in engineering practice or research, but have found merit in previous studies (Mohssen, 2009; Papalexiou et al., 2013). As a result, this study incorporated the distributions as an exploratory case to better understand if the October 2015 flood shifted the tail behavior of maxima towards a heavier tail distribution. In the case where the limiting form is an excess distribution, such as the GP or PP, comparative annual design quantiles were estimated by considering the threshold exceedance rate and number of raw observations per year (Coles, 2001) and therefore can be practically applied in the infrastructure design setting. The supporting parameterization of the cumulative distribution and their inherent parameters implemented within the study are provided in Table 1.

Table 1. Probability distributions used in this study.

Model	Cumulative Distribution Function (CDF)	Parameters	Reference
GEV	$F(x) = \begin{cases} \exp\left\{-\left[1+\xi\left(\frac{x-\mu}{\sigma}\right)\right]^{-1/\xi}\right\}, & \xi \neq 0 \\ \exp\left(-\exp\left(\frac{\mu-x}{\sigma}\right)\right), & \xi = 0 \end{cases}$	μ = location σ = scale ξ = shape	Jenkinson, 1955; von Mises, 1936; Gumbel, 1958
Gumbel	$F(x) = \exp\left(-\exp\left(\frac{\mu-x}{\sigma}\right)\right)$	μ = location σ = scale	Jenkinson, 1955; von Mises, 1936; Gumbel, 1958
GP	$F(y) = \begin{cases} 1-\left(1+\xi\frac{y}{\tilde{\sigma}}\right)^{-1/\xi}, & \xi \neq 0 \\ 1-\exp\left(\frac{-y}{\tilde{\sigma}}\right), & \xi = 0 \end{cases}$	y = x – u (threshold excess) $\tilde{\sigma}$ = modified scale ξ = shape	Pickands III, 1975; Balkema and de Haan, 1974; Coles, 2001
PP	$\Lambda(A) = (t_2 - t_1)\left[1+\xi\left(\frac{x-\mu}{\sigma}\right)\right]^{-1/\xi}$	μ = location σ = scale ξ = shape	Leadbetter et al., 1983; Resnick, 1987; Smith, 1989; Davison and Smith, 1990; Coles, 2001

A fair comparison between various fitting models requires the assessment of the uncertainty of probabilities, return periods, and design quantiles. Indeed, when evaluating design properties, the differences of modeling estimates should be significant for operational use. In this respect, there are several methodologies that have recently been applied to various extreme fitting models including the delta method (Obeysekera and Salas, 2014), the bootstrap resampling method (Efron and Tibshirani, 1993; Samadi, et al., 2013), and the profile likelihood function method (Obeysekera and Salas, 2014).

The delta method relies on the asymptotic properties of the maximum likelihood estimates of the model parameters and their covariance matrix (e.g., Serinaldi and Kilsby, 2014; Obeysekera and Salas, 2014). It calculates symmetric CIs under the hypothesis that the distribution of the quantiles is reasonably described by a Gaussian distribution. The bootstrap method resamples the observed series using nonparametric bootstrapping or parametric bootstrapping (also so-called Monte Carlo simulation) to

simulate iid realizations of a random variable *Y* and to draw a suitable standardized distribution. The bootstrap method provides an assessment of the sampling and parameter estimation uncertainties by realistic asymmetric CIs (Serinaldi and Kilsby, 2014). Unlike the bootstrap method, the profile likelihood function relies on the asymptotic properties of maximum likelihood estimators, although this method is difficult to implement and can be quite computationally burdensome (e.g., Obeysekera and Salas, 2014). In this study, the bootstrap method is used to calculate the uncertainty of CIs because it is independent of the probability estimation method and provides more reliable simulation of iid realization.

3.2. Parameter Estimation

The method of moments and method of L-moments have been traditionally employed to estimate distribution parameters in hydrological datasets (Hosking et al., 1985; Maidment, 1993; Gubareva and Gartsman, 2010). In recent years, due to advancements in computing, the method of maximum likelihood estimation (MLE) and generalized MLE (GMLE) (Martins and Stedinger, 2000, 2001) have a growing interest. These methods provide unbiased parameter estimates compared to the method of moments, thus the MLE method was adopted for the estimation of distribution parameters for the results presented herein.

Table 2. Model likelihood functions.

Model	Likelihood Function	Condition
GEV	$\ell(\mu,\sigma,\xi) = -m\log\sigma - (1+1/\xi)\sum_{i=1}^{m}\log\left[1+\xi\left(\frac{z_i-\mu}{\sigma}\right)\right] - \sum_{i=1}^{m}\left[1+\xi\left(\frac{z_i-\mu}{\sigma}\right)\right]^{-1/\xi}$	$1+\xi\left(\frac{z_i-\mu}{\sigma}\right)>0, for\ i=1,\dots,m$
Gumbel	$l(\mu,\sigma) = -m\log\sigma - \sum_{i=1}^{m}\left(\frac{z_i-\mu}{\sigma}\right) - \sum_{i=1}^{m}\exp\left\{-\left(\frac{z_i-\mu}{\sigma}\right)\right\}$	$\xi=0$
GP	$l(\tilde{\sigma},\xi) = -k\log\tilde{\sigma} - (1+1/\xi)\sum_{i=1}^{k}\log(1+\xi\, y_i/\tilde{\sigma})$ $l(\tilde{\sigma}) = -k\log\tilde{\sigma} - \tilde{\sigma}^{-1}\sum_{i=1}^{k} y_i$	$1+\tilde{\sigma}^{-1}\xi y_i>0\ for\ i=1,\dots,k$ $\xi=0$
PP	$l(\mu,\sigma,\xi) = -\log\sigma - \left(1+\frac{1}{\xi}\right)\sum_{i=1}^{n_u}\log\left[1+\xi\left(\frac{x_i-\mu}{\sigma}\right)\right] - n_y\log\left[1+\xi\left(\frac{x_i-\mu}{\sigma}\right)\right]$	$1+\xi\left(\frac{x_i-\mu}{\sigma}\right)>0, for\ i=1,\dots,n_u$

For the case where the random variable, x, has probability density function, $f(x;\theta_0)$, the likelihood function is given as

$$L(\theta) = \prod_{i=1}^{n} f(x_i;\theta). \tag{4}$$

Equation (4) represents the likelihood function of a set of independent realization of the random variable, x, given a set of parameters, θ, which describes the underlying nature of the probability density function (Coles, 2001). Usually the optimization of the parameter set is addressed in terms of the log-likelihood function given by

$$l(\theta) = \log L(\theta) = \sum_{i=1}^{n} \log f(x_i; \theta). \quad (5)$$

During the maximum likelihood approach, Equation (5) is implemented using optimization procedures such that the log-likelihood function is maximized resulting in the maximum likelihood estimates of the distribution parameter set, θ. Because of the monotonic behavior of the log-likelihood function, the likelihood and log-likelihood functions take on the maximum given the same set of likelihood estimators (Coles, 2001). The model likelihood functions implemented within this study are outlined in Table 2.

3.3. Threshold Selection

A critical component in the implementation of the GP and PP excess distribution models in hydrological frequency analysis is the selection of a threshold value (Villarini et al., 2011; Saeed Far and Wahab, 2016). In this study, mean residual life plots and threshold range plots (Coles, 2001) were applied for the evaluation of threshold values. Each of these exploratory techniques aim to guide in the selection of a minimum threshold such that there is linearity below the threshold in the mean residual life plot and there is stability beyond the threshold in the distribution parameters (Coles, 2001; Saeed Far and Wahab, 2016). Further evaluation of threshold selection for the POT and its influence on the performance of the GP and PP models was analyzed by taking into consideration the significance level for the goodness of fit tests outlined earlier.

In this study, threshold values were selected such that appropriate significance levels were achieved with the lowest possible threshold as to limit the resulting variance in distribution parameter estimation, while achieving agreement among the three goodness of fit two-sided p-values. Each of the above techniques was employed, along with goodness of fit tests (Kolmogorov–Smirnov (K-S), Cramer–von Mises (C-vM), and Anderson–Darling (A-D)), to derive a threshold value for each USGS gauging station. It is

important to note that in the case of block maxima data, the threshold value was set slightly lower than the absolute minimum of the AMF data set such that all events are considered. This is done because by nature, that is the natural threshold of the AMF time series. As a result, the GP and PP distributions consider the AMF data in the same facet as the GEV and Gumbel distributions, thereby providing consistent sample sizes for which the distribution parameters can be estimated and prevent additional bias.

4. Applications

4.1. Analysis of Rocky Creek

Rocky Creek drains approximately 502.5 square kilometers (sqkm) just north of the Catawba River into Lake Wateree, SC. The drainage area above the USGS monitoring station can be classified as moderately rural, composed of smaller communities and residential areas. In this drainage system, the peak flow rate during the October 2015 flood event was approximately 59 cubic meters per second (cms), with a sustained peak rate for approximately 8 hours.

Analysis begins with the diagnostic plots. Figure 3a presents the results for the fitted cumulative distribution function, P-P (probabilities plot), and Q-Q (quantile-quantile) plots for the GEV, GP, Gumbel, and PP models using historical AMF records without the inclusion of the 2015 flood event (i.e., 1952-2015). For clarity, these data will be referred to as AMF herein, while historical records with the 2015 event will be referred to as AMF-2015. The diagnostic plots reveal that both the GEV and the Gumbel models more precisely predicted the empirical distribution and probabilities when compared to the GP and the PP models. Both the GEV and Gumbel distributions appeared to have comparable quantile accuracy below 250 cms, with the GEV model showing more variability in its upper tail bound. Visual fitting results of the GP and PP models indicate that each model under/over predicted the observed probability (P-P) and increasingly deviated from the observed quantiles with increasing probabilities.

A more detailed review of the fitting performance data provides a summary of the four models for the AMF data. Table 3 presents two-sided p-values for the K-S, C-vM, and A-D tests, the Pearson correlation coefficient (ρ), P-P coefficient of determination (R^2), AIC, and BIC. The upper tail performance of the GEV model as indicated by the A-D test proves a slightly higher significance compared to the Gumbel model, while the overall fitting performance indicated by the K-S test is much lower than that of the Gumbel. The cumulative consideration of the goodness of fit test results and the information-based criteria indicated that the Gumbel distribution provided the best fit for the Rocky Creek AMF data followed by the GEV, GP, and PP models, respectively. It is important to note that the selection of the most appropriate parent distribution within this study was based on the distribution which produced the highest and most consistent significance level (i.e., two-sided p-value) for the K-S, C-vM, and A-D tests, while also generating the lowest information-based criteria set forth by the AIC and BIC statistics.

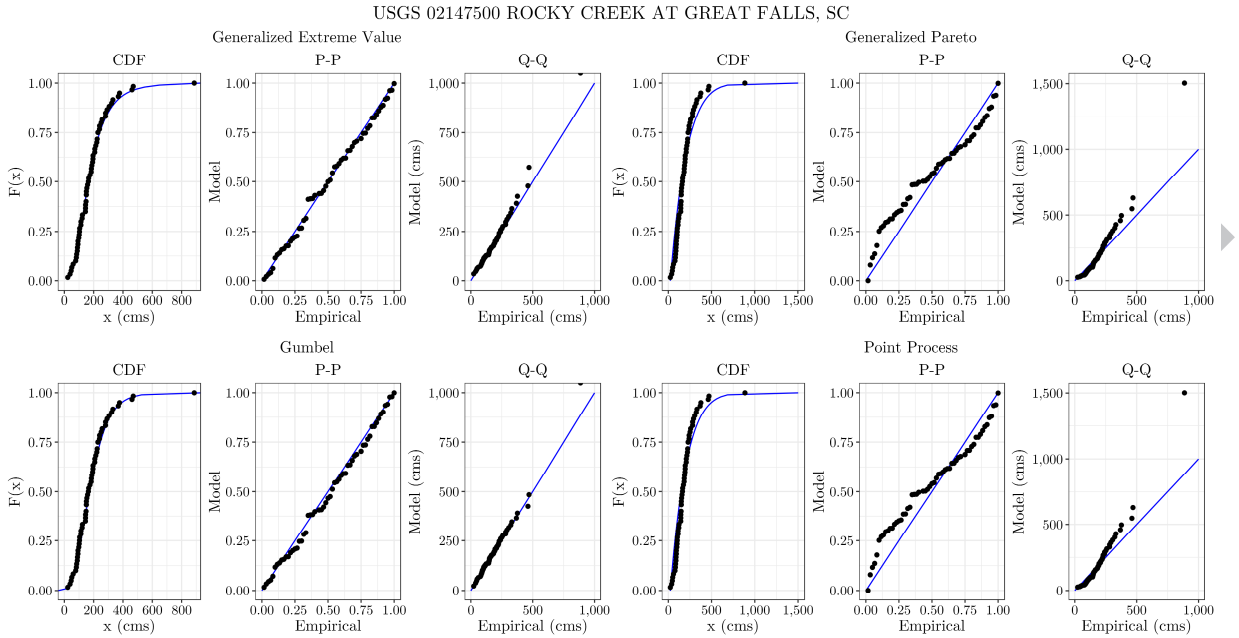

(a)

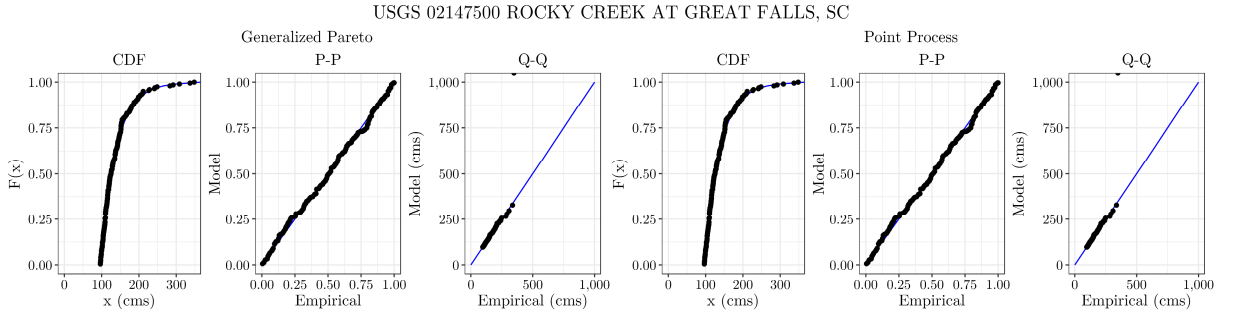

(b)

Figure 3. Rocky Creek diagnostic plots: (a) AMF series and (b) POT series.

Next, the analysis proceeded using AMF-2015 data. Results of the AMF-2015 analysis are based on the hypothesis that the parent distribution of AMF (i.e., Gumbel) would not hold true for AMF-2015. Inclusion of the 2015 flood event within the AMF dataset (i.e., AMF-2015) served as an investigatory analysis into the underlying evaluation of the potential abnormality of the 2015 hurricane event and its impact on the underlying parent distribution of AMF. Referring to Table 3, the performance of the probability models was not generally affected when including the October 2015 flood event. However,

the fitted models of the EVT family showed slightly asymmetric behavior, but they were not prominent as the upper tails of GP, GEV, and PP models are approximately exponential (i.e., their shape parameters are close to zero). In this respect, the Gumbel model deemed more accurate than those obtained by power law. As expected, the only model which experienced a significant impact on performance was the GEV (K-S > 0.05).

Table 3. Rocky Creek AMF performance summary.

Without 2015 Flood Event							
Model	K-S[1]	C-vM[1]	A-D[1]	Pearson (ρ)	R^2	AIC	BIC
GEV	0.8599	0.9886	0.9971	0.9977	0.9946	728.5	734.8
GP	0.0627	0.0629	0.0529	0.9862	0.9229	738.5	742.7
GUMBEL	**0.9942**	**0.9773**	**0.9751**	**0.9978**	**0.9909**	**729.9**	**734.1**
PP	0.0626	0.0630	0.0530	0.9862	0.9229	860.5	866.8
With 2015 Flood Event							
Model	K-S[1]	C-vM[1]	A-D[1]	Pearson (ρ)	R^2	AIC	BIC
GEV	0.8071	0.9770	0.9948	0.9972	0.9938	726.6	732.9
GP	0.0884	0.0737	0.0627	0.9867	0.9277	735.7	739.9
GUMBEL	**0.9892**	**0.9701**	**0.9613**	**0.9977**	**0.9904**	**728.5**	**732.7**
PP	0.0882	0.0736	0.0626	0.9867	0.9277	857.7	864.0

[1]Two sided p-value.

The fitted distribution parameters presented in Table 4 highlight the superiority of the Gumbel model for the AMF-2015 series. When compared to the rest of the models, the Gumbel distribution computed the second lowest scale parameter, thus constituting a much lower variance in the predicted runoff level for any given design period. This result indicates that the hurricane event more so follows the underlying distribution of the annual flood data, rejecting the hypothesis of power law distribution for the Rocky Creek AMF-2015 dataset.

Table 4. Rocky Creek AMF distribution parameters.

	Without 2015 Food Event				With 2015 Flood Event			
Parameter	GEV	GP	**GUMBEL**	PP	GEV	GP	**GUMBEL**	PP
Location[1]	134.52	23.13	**141.27**	23.11	130.11	23.13	**137.30**	23.16
Scale[2]	78.36	190.43	**83.89**	190.46	76.55	183.73	**82.67**	183.68
Shape	0.1469	-0.1286	**-**	-0.1288	0.1602	-0.1159	**-**	-0.1157

[1]Threshold for the GP model
[2]Modified scale for the GP model

As the second part of data analysis for Rocky Creek, a continuous time series (i.e., sub-hourly) of DMF was extracted for a period from 10/01/1986 – 09/30/2015. GP and PP are the two most appropriate distributions to describe the exceedance over threshold, thus they were implemented for POT probability analysis. Diagnostic plots of the resulting POT frequency analysis without the inclusion of the 2015 flood (i.e., POT) are presented in Figure 3b. Examination of the CDF and P-P plots suggest a decreased performance in the parent distribution (i.e., Gumbel), due to the variation between the model and observed data. An assessment of the GP and PP diagnostic plots show arguably exceptional fits, with a very fine degree of variation between the model and observed data, with little-to-no visual deviance between the two model results.

Overall, the GP and PP models provided between 0.85 and 0.93 significance levels, with a well computed upper tail bound (i.e., A-D ≈ 0.93). The GP and PP models generated nearly identical results given the goodness of fit tests and coefficient of determination, but the PP model dominated after review of the Bayesian information criteria. Inclusion of the 2015 flood event (i.e., POT-2015) appeared to have a marginally significant effect on the central distribution behavior as indicated by the K-S test. However, the upper tail behavior outlined by the A-D significance levels showed negligible impact.

Table 5 - Rocky Creek POT performance summary.

Without 2015 Flood Event							
Model	K-S[1]	C-vM[1]	A-D[1]	Pearson (ρ)	R^2	AIC	BIC
GP	0.8552	0.9081	0.9352	0.9991	0.9975	1,887.0	1,893.5
PP	**0.8545**	**0.9076**	**0.9348**	**0.9991**	**0.9975**	**1,520.2**	**1,530.1**
With 2015 Flood Event							
Model	K-S[1]	C-vM[1]	A-D[1]	Pearson (ρ)	R^2	AIC	BIC
GP	0.7964	0.9195	0.9453	0.9990	0.9975	1,942.2	1,948.9
PP	**0.7961**	**0.9199**	**0.9456**	**0.9990**	**0.9975**	**1,560.4**	**1,570.3**

[1]Two sided p-value.

The resulting distribution parameters for the POT analysis are presented in Table 6. The PP model distribution parameters for the POT with the 2015 event clearly show an increase. For example, the variation in predicted runoff, as indicated by the scale parameter, increased from 43.4 cms to 45.9 cms, while the rate at which runoff generation grows with more intense events, set forth by the shape parameter, increased from 0.017 to 0.031. Although the increase in the parameters is small, the increase in the positive shape parameter indicates the possibility of the return level growth and non-linear increase over larger return periods. Thus, the inclusion of additional data within the POT time series appears to have a considerable effect, to a degree, of the ultimate distribution shape and hence the underlying vulnerability of current drainage infrastructure.

Table 6. Rocky Creek POT distribution parameters.

	Without 2015 Food Event		**With 2015 Flood Event**	
Parameter	GP	**PP**	GP	**PP**
Location[1]	96.28	**178.76**	96.28	**183.20**
Scale[2]	42.03	**43.40**	43.23	**45.91**
Shape	0.0163	**0.0167**	0.0312	**0.0306**

[1]Threshold for the GP model
[2]Modified scale for the GP model

Addressing the implications of the flood event through the AMF and POT analysis was complimented by return level predictions generated from the AMF and POT parent distribution parameters. These estimates with the bootstrapped 95% CIs are presented in Figure 4. The results indicate that the BM's parent distribution replicated the theoretical return level function quite well (see raw data points). The AMF computed return levels from the Gumbel distribution had little-to-no dispersion below the 25-year return period. Unlike the AMF, the POT return model had much more variation between the modeled and empirical results. Since the annual time series was best represented with a Gumbel model, there is a strong linearity in return level estimation, with less uncertainty above the 50-year level when compared to the POT model (i.e., PP distribution).

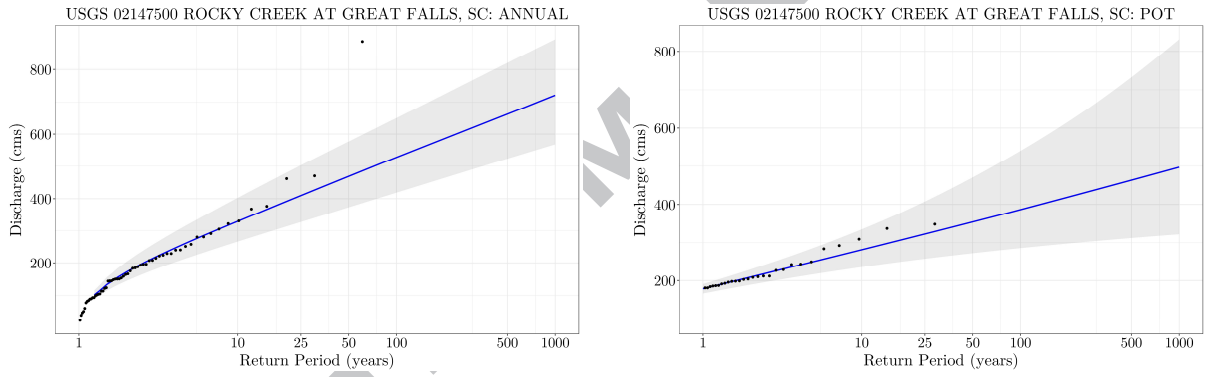

(a) **(b)**

Figure 4. Computed return levels for Rocky Creek excluding the 2015 flood event for (a) AMF and (b) POT. Bootstrap 95% confidence intervals are shown as the shaded region.

The width of the CIs confirms that a large uncertainty characterizes the results obtained by the POT analysis. For instance, the AMF 100-year return level ranged between approximately 420 to 650 cms, whereas a significant width of the CI for lower (i.e., 10-year) and upper (i.e., > 100-year) return levels reflect that the model is less informative. This further implies that the increase of extreme data is paid in terms of the increase of uncertainty and extreme complexity. In both cases, the shape and underlying distribution were different. However, a peak flow rate of 59 cms only registered as a 1.1-year and 1.0-

year return period for the AMF and POT model, respectively, thus confirming that the 2015 hurricane event cannot be classified as an extreme event from a truly probabilistic point of view.

4.2. Analysis of the Enoree River

The Enoree River lies in the heart of the Sumter National Forest draining more than 1,150 sqkm of rural and urban land and eventually discharging into the Broad River. Available historical datasets for this basin provided AMF data from 1974-2015, in addition to continuous (i.e., sub-hourly) flow data from 04/05/1985 – 09/30/2015.

Figure 5a presents the diagnostic plot results of the AMF analysis. The results indicate that the GEV and Gumbel models appeared to be good indicators for predicting the annual maxima, with little deviation between model and empirical estimates. The CDF plots of these models show similar characteristics in the lower tail behavior of the distribution, but a review of the probability plots reveals that the GEV had much less variation between the model and the observed data than that of the Gumbel. The quantile plots confirm this result and show that the GEV model had more accuracy in predicting the upper tail behavior of the AMF distribution when compared to the Gumbel. A significant increase in the shape parameter of AMF-2015 denotes a tendency to heavier tailed Fréchet law. Unlike the GEV model, both the GP and PP resulted in slight deviations in the model fitting.

The AMF results (Table 7) showed a superior performance of the GEV model for all goodness of fit results (≈ 0.87 to 0.90). However, each of the models proved to have similar accuracy in predicting the probability of exceedance, with the GEV being however the most realistic among the competitors. As illustrated by the diagnostic plots (see Figure 5a), the Gumbel model represented the distribution of data well, but falls short of the GEV with significance levels approximately 0.22 to 0.42 lower than the GEV. The central tendency of the GP and PP models was slightly lower than that of the Gumbel, nonetheless the tail performance was at most satisfactory (≈ 0.16). The consideration of each of the performance

standards led to the adoption of the GEV model as a proxy for the AMF data. However, interestingly, the GEV, GP, and PP models had similar Bayesian criterion with the latter being the most realistic model.

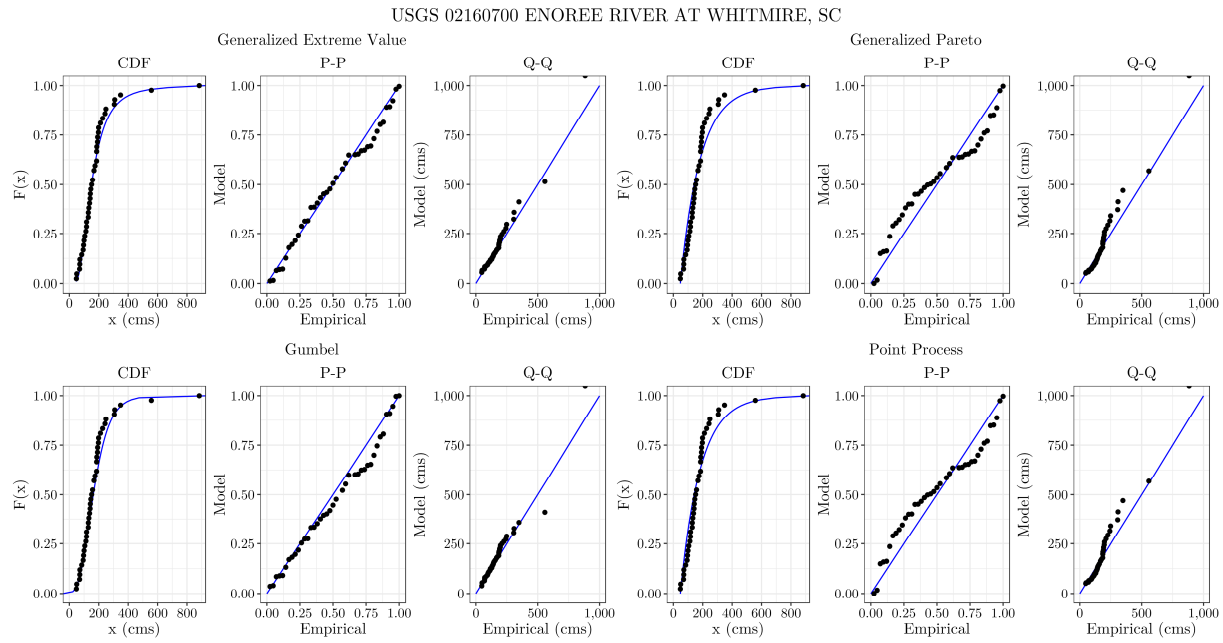

(a)

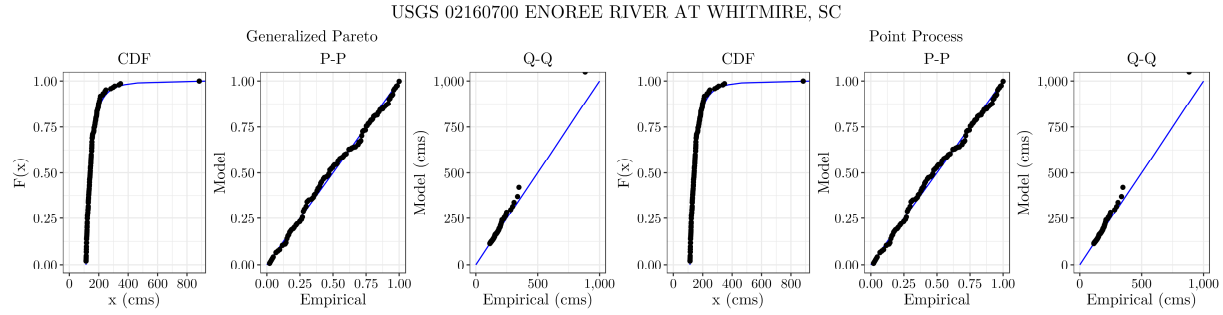

(b)

Figure 5. Enoree River diagnostic plots: (a) AMF series and (b) POT series.

Including the 2015 flood event within the AMF dataset (i.e., AMF-2015) predominantly affected the GEV and the Gumbel models, although around the 5% significance level. In both cases, the performance of the goodness of fit tests improved, with the most improvement observed in the tail behavior of the

distributions. For example, prior to the 2015 hurricane, the A-D statistic for the GEV model was 0.90, while following the event this statistic increased to approximately 0.95. Improved performance was also noted in the GP and PP models, although affected less than the 2% CI. As a result, the GEV model maintained the stance of representing the AMF distribution. However, as Cooley, 2013 stated, any method for generating CIs has drawbacks, therefore, caution should be exercised when interpreting such results.

A review of the fitted distribution parameters is warranted to further summarize the response of the probability distribution to the 2015 flood event. The results presented in Table 8 do not suggest a larger rate of variability of the runoff prediction for the GEV, GP, and PP models, as indicated by the shape parameter. However, the GP and PP models did tend to show much more fluctuation in the model when comparing the scale parameter during pre- and post-hurricane event. For instance, the GEV model showed an increase in the scale parameter of approximately 1.6 cms, while the GP and PP models increased by approximately 5 cms. In this basin, incorporation of AMF excess models (i.e., GP and PP) presented more uncertainty in design variables as opposed to the selected GEV parent distribution.

Table 7. Enoree River AMF performance summary.

Without 2015 Flood Event							
Model	K-S[1]	C-vM[1]	A-D[1]	Pearson (ρ)	R^2	AIC	BIC
GEV	**0.8726**	**0.8653**	**0.9092**	**0.9938**	**0.9844**	**498.9**	**504.1**
GP	0.3289	0.1595	0.1624	0.9770	0.9282	501.4	504.9
GUMBEL	0.4540	0.6492	0.5701	0.9925	0.9653	505.0	508.5
PP	0.3277	0.1592	0.1621	0.9770	0.9281	587.4	592.6
With 2015 Flood Event							
Model	K-S[1]	C-vM[1]	A-D[1]	Pearson (ρ)	R^2	AIC	BIC
GEV	**0.9150**	**0.9138**	**0.9476**	**0.9949**	**0.9872**	**512.6**	**517.9**
GP	0.3468	0.1772	0.1793	0.9796	0.9343	515.0	518.5
GUMBEL	0.4948	0.6946	0.6327	0.9931	0.9689	518.3	521.8

PP	0.3474	0.1774	0.1795	0.9796	0.9343	603.0	608.2

[1]Two sided p-value.

The distribution fitting performance increased with the addition of the 2015 hurricane event. However, many of the estimated distribution parameters experienced a slight increase. For example, the GEV location and scale parameters increased by approximately 2 cms and 1.6 cms, respectively, while the shape parameter remained constant. In this regard, the central tendency and the anticipated variation of the discharge increase, such an increase is considered minor and practically immeasurable in engineering practice. Most importantly, the upper tail behavior (i.e., shape parameter) of the distribution remained unchanged by the hurricane event. As a result, the parent distribution did not show significant deviations during the post-event analysis, indicating no abnormalities or outlier prone evidence of the 2015 hurricane event in this drainage system. It is however important to note that the lack of abnormalities indicated by the distribution performance and parameters does not necessarily negate the potential extreme intensity of the event.

Table 8. Enoree River AMF distribution parameters.

	Without 2015 Food Event				**With 2015 Flood Event**			
Parameter	**GEV**	GP	GUMBEL	PP	**GEV**	GP	GUMBEL	PP
Location[1]	**126.24**	47.83	136.00	47.80	**128.27**	47.83	138.07	47.81
Scale[2]	**63.35**	134.84	73.48	134.76	**64.99**	139.26	75.01	139.31
Shape	**0.2489**	0.0180	-	0.0180	**0.2452**	0.0049	-	0.0047

[1]Threshold for the GP model
[2]Modified scale for the GP model

Further evaluation of the extremeness of the 2015 flood event was continued for the Enoree River with the development of probability models using the partial duration series prior to the 2015 flood event. Visual inspection of the diagnostic plots for these models (Figure 5b) indicated exceptional fits for both the GP and PP in terms of the predicted distribution function (i.e., CDF). The results of goodness of fit tests revealed that the GP model simply provides a proxy for the probabilities of exceedance *Qi*, with the PP model trailing. However, Bayesian statistics highlight the superiority of the PP model (see Table 9).

Table 9. Enoree River POT performance summary.

Without 2015 Flood Event							
Model	K-S[1]	C-vM[1]	A-D[1]	Pearson (ρ)	R^2	AIC	BIC
GP	0.8218	0.7737	0.8474	0.9974	0.9947	1,402.0	1,407.9
PP	**0.8231**	**0.7748**	**0.8480**	**0.9974**	**0.9947**	**1,238.0**	**1,246.9**
With 2015 Flood Event							
Model	K-S[1]	C-vM[1]	A-D[1]	Pearson (ρ)	R^2	AIC	BIC
GP	0.9374	0.8863	0.9403	0.9981	0.9962	1,454.3	1,460.3
PP	**0.9362**	**0.8851**	**0.9398**	**0.9981**	**0.9962**	**1,277.9**	**1,286.9**

[1]Two sided p-value.

Evaluation proceeded by analysis of the POT-2015 series. The results presented in Table 9 prove that the inclusion of the 2015 flood event significantly affected the distribution performance. Both the GP and PP models show improvement in model adequacy. In the case of the POT-2015 analysis, it appears the hurricane event significantly affected the parent distribution in terms of the goodness of fit tests. However, both the GP and PP models showed little-to-no degree of variability in the distribution parameters (see Table 10). The most adequate fit, the PP model, showed the highest increase in the estimated scale and shape parameters when compared to the GP distribution.

Table 10. Enoree River POT distribution parameters.

	Without 2015 Flood Event		**With 2015 Flood Event**	
Parameter	GP	**PP**	GP	**PP**
Location[1]	113.27	**180.91**	113.27	**185.60**
Scale[2]	32.94	**54.97**	34.32	**58.30**
Shape	0.3258	**0.3255**	0.3312	**0.3317**

[1]Threshold for the GP model
[2]Modified scale for the GP model

Figure 6 shows the 95% CIs obtained by the GEV and PP models for the AMF and POT data sets, respectively. In both cases, the predicted return levels for lower return periods (i.e., < 25-year event) showed close to each other, though a high variability existed at higher frequencies between two

formulations. Further, both series CIs were slightly asymmetric and deemed more accurate based on performance criterion. However, such asymmetry was more prominent for the POT model, as the upper tail of the PP distribution was not exponential (i.e., the GEV shape parameter is not close to zero). The fitted model for POT indeed showed more nonlinear temporal patterns compare to the AMF. As illustrated, the width of the CIs of higher frequencies/return periods confirms that a significant uncertainty characterizes the results obtained by the PP distribution. This further demonstrates that the increase in model complexity (i.e., moving from GEV to PP distribution) is paid in terms of increasing uncertainty and more complex probability models cannot replace information if this is not available.

Estimated return periods for the Enoree River discharge (i.e., 303 cms) during the 2015 event were 8.8 years and 5.8 years for the AMF and POT datasets, respectively. The modeled return periods show larger intensities compared to the previous application, but still much lower than typical bridge and road design settings in the study region (i.e., ≥ 25-year return period). Although the POT distribution fit and parameter values did experience more significant variations when compared to the AMF analysis, these results corroborate and substantiate the previous FFA results and provide reason to disregard the runoff event as a truly extreme sample from the underlying distribution of flood events.

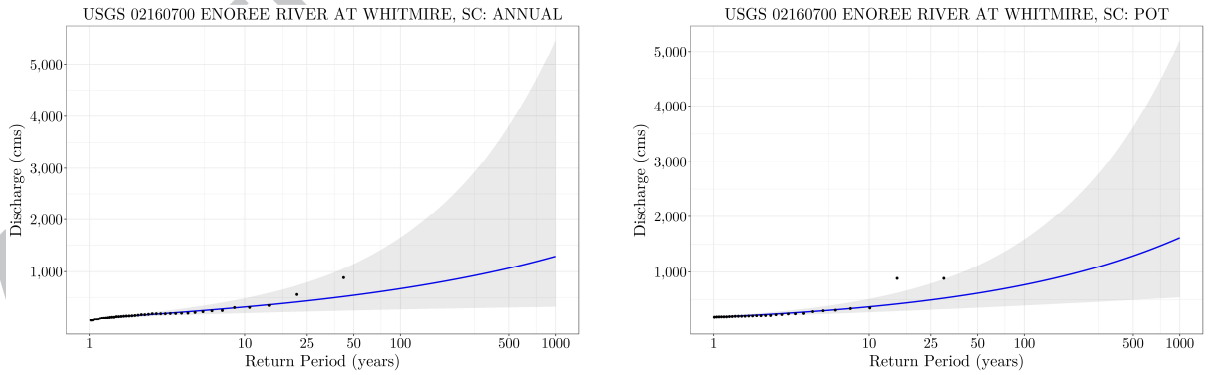

(a) **(b)**

Figure 6. Computed return levels for the Enoree River excluding the 2015 flood event for (a) AMF and (b) POT. Bootstrap 95% CIs are shown as the shaded region.

4.3. Analysis of the Saluda River

The Saluda River is situated below Lake Greenwood, draining a diverse set of landscapes and river systems totaling more than 3,522 sqkm and eventually discharging to Lake Murray outside of Lexington, SC. Due to the size and slope of the Saluda River basin, a maximum peak flow of nearly 1,000 cms was recorded to have caused considerable damages to water control structures (e.g., dams and ponds) during hurricane Joaquin. The USGS station at the Saluda River monitors flow since 1906 (i.e., 108-year data set for BM). However, a continuous sub-daily maximum flood data set is not readily available until 07/31/1986.

Diagnostic plots for the AMF series are shown in Figure 7a. As illustrated, the GP and PP modeled adequately in terms of predicting most of the observed flood data when compared to the GEV and the Gumbel models. Inspection of the P-P plots show each model had a degree of dispersion, with the GP and PP being less biased. A review of the Q-Q plots reveals the effectiveness of the GP and PP models in all cases apart from the single most extreme flood event, a much different result from the previous applications of the Rocky Creek and the Enoree River basins. For example, the GP and PP models showed an excellent fit to the observed discharge levels below approximately 1,700 cms, although in some intervals the models over predicted large flood events. The Gumbel distribution visually appeared to offer the most concise quantile estimates (i.e., less dispersion) when compared to empirical data.

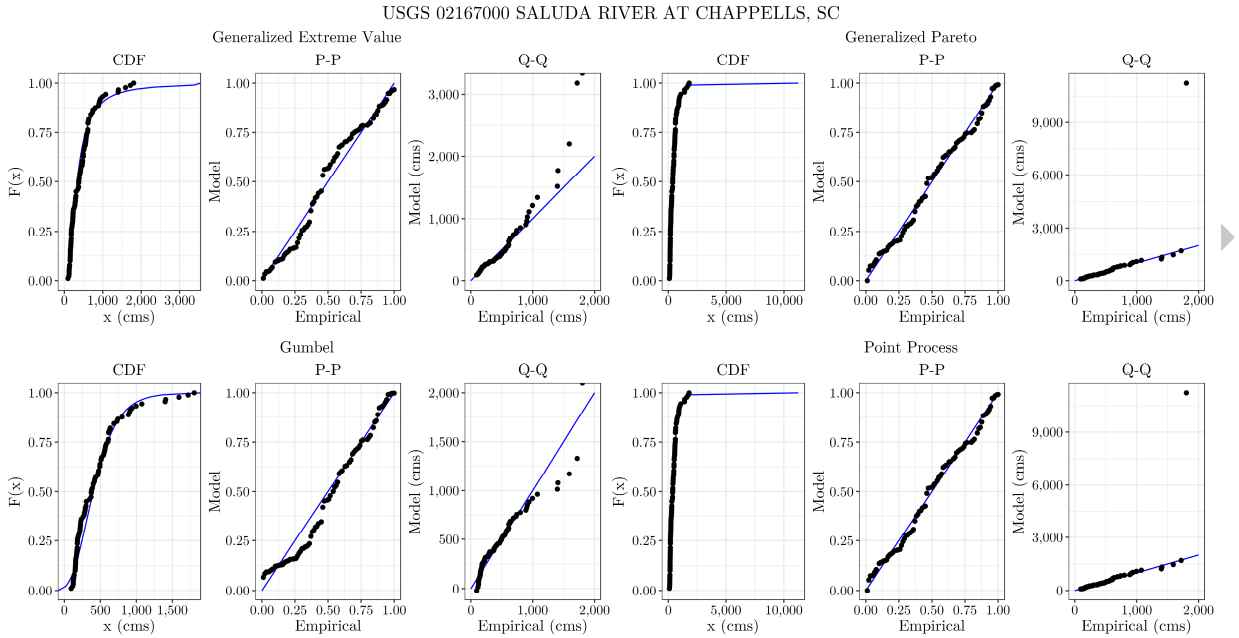

(a)

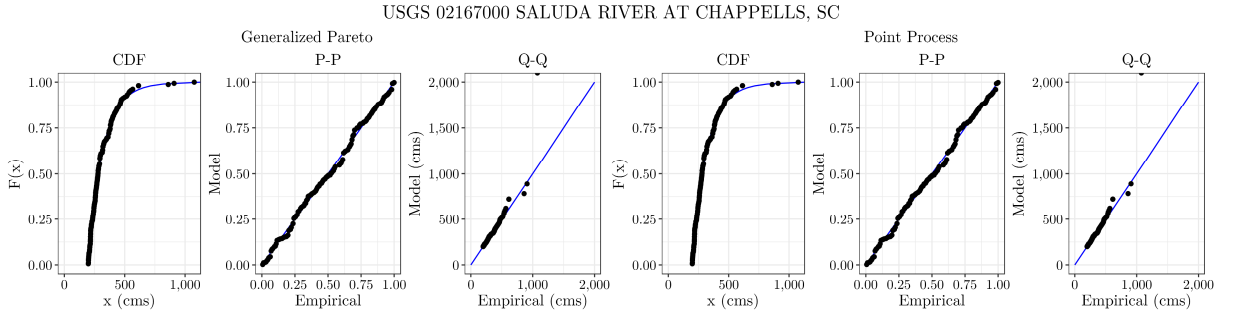

(b)

Figure 7. Saluda River diagnostic plots: (a) AMF series and (b) POT series.

Inspection of the performance indicators (Table 11) of the four probability models show that the GP model outperformed the PP model, followed by the GEV and Gumbel, respectively. Unlike the two previous applications, the GP and PP statistical significance of the fits, as indicated by the K-S, C-vM, and A-D two-sided p-values, were substantially higher (i.e., ≈ 0.70 to 0.93 significance levels). Statistically, the GEV model did provide evidence that the flood data could come from the distribution, with confidence levels of approximately 0.24 to 0.30. However, the selected parent distribution of the GP

had more than twice the confidence level. Similarly, the Gumbel did show minor confidence in the distribution of the flood data, but with satisfactory results in the tail estimate around 0.11.

Extension of the annual time series to include the 2015 flood event (i.e., AMF-2015) is summarized in Table 11. The performance summary results did not change significantly for the GEV and Gumbel models. However, the GP and PP models experienced a slight improvement in the overall fitting. The fitted distribution parameters (Table 12) substantiate this hypothesis, although there was an increased degree of variability introduced into each model. For example, the GP model most appropriately represented the behavior of annual extreme events for the Saluda River basin. Inclusion of the 2015 flood event within the AMF series increased the scale parameter by nearly 11 cms. In this case, a larger degree of uncertainty in the estimated runoff is present when compared to the previous applications, especially at larger runoff rates.

Table 11. Saluda River AMF performance summary.

Without 2015 Flood Event							
Model	K-S[1]	C-vM[1]	A-D[1]	Pearson (ρ)	R^2	AIC	BIC
GEV	0.3032	0.2482	0.2939	0.9887	0.9731	1,246.3	1,253.7
GP	**0.9375**	**0.7702**	**0.7034**	**0.9956**	**0.9906**	**1,235.4**	**1,240.4**
GUMBEL	0.1228	0.2143	0.1163	0.9885	0.9651	1,262.7	1,267.7
PP	0.9371	0.7701	0.7034	0.9956	0.9906	1,415.4	1,422.9
With 2015 Flood Event							
Model	K-S[1]	C-vM[1]	A-D[1]	Pearson (ρ)	R^2	AIC	BIC
GEV	0.3012	0.2474	0.2888	0.9889	0.9734	1,263.6	1,271.1
GP	**0.9532**	**0.7900**	**0.7318**	**0.9958**	**0.9910**	**1,251.9**	**1,256.9**
GUMBEL	0.1214	0.2108	0.1161	0.9886	0.9652	1,279.5	1,284.5
PP	0.9531	0.7899	0.7318	0.9958	0.9910	1,433.9	1,441.4

[1]Two sided p-value.

In addition, the block maxima approach yielded much more appropriate performance for the GP and PP models in comparison to the GEV and Gumbel models. However, the small size of the samples, usually less than 50 AMF, tends to hide the heavy tail behavior as seen elsewhere (e.g., Serinaldi and Kilsby, 2014, 2015). Evaluation of the frequency analysis using partial duration series led to a more abundant supply of extreme data points, although over only a portion of the annual period of record. Hence, the threshold models (i.e., GP and PP) provided superiority over the rest of the models.

Table 12. Saluda River AMF distribution parameters.

	Without 2015 Food Event				**With 2015 Flood Event**			
Parameter	GEV	**GP**	GUMBEL	PP	GEV	**GP**	GUMBEL	PP
Location[1]	265.31	**94.55**	319.03	94.65	268.25	**94.55**	322.86	94.50
Scale[2]	165.21	**384.84**	225.67	384.72	168.56	**395.20**	229.51	395.14
Shape	0.5158	**-0.0346**	-	-0.0345	0.5147	**-0.0465**	-	-0.0463

[1]Threshold for the GP model
[2]Modified scale for the GP model

Figure 7b presents the diagnostic plots for the extreme value distributions considered for the Saluda River POT time series. Like the block maxima dataset, the GP and PP models characterized the extreme flood events well below the 90% exceedance level, while overpredicting events above this threshold. Further investigation of the GP and PP probability plots revealed a less degree of dispersion when compared to the AMF results (Figure 7a). Moreover, the POT frequency analysis slightly affected the central tendency of the probability models. However, the upper tail performance was significantly affected by this frequency approach (Table 13). For example, the AMF analysis resulted in approximately 70% CIs for the upper tail behavior of the GP model (i.e., A-D), while POT yielded a 95% significance level for the adequacy of the GP model based on the goodness of fit test.

Considering different goodness of fit statistics, the PP model provided the best overall fit, although the effect on the upper tail behavior was negligible. The results presented in Table 13 show that 2015 flood

event appeared to have a marginally significant effect (i.e., ≈ 5%) on the overall performance of the POT models. For example, the A-D test prior to the 2015 event was estimated at 0.9504, while the test results with the hurricane event produced a significance level of 0.9532. Therefore, the inclusion of the 2015 flood data appears to be less statistically significant.

Table 13. Saluda River POT performance summary.

Without 2015 Flood Event							
Model	K-S[1]	C-vM[1]	A-D[1]	Pearson (ρ)	R^2	AIC	BIC
GP	0.8607	0.9292	0.9504	0.9984	0.9966	1,834.4	1,840.6
PP	**0.8608**	**0.9291**	**0.9504**	**0.9984**	**0.9966**	**1,611.4**	**1,620.6**
With 2015 Flood Event							
Model	K-S[1]	C-vM[1]	A-D[1]	Pearson (ρ)	R^2	AIC	BIC
GP	0.9098	0.9385	0.9532	0.9985	0.9967	1,890.9	1,897.1
PP	**0.9119**	**0.9385**	**0.9532**	**0.9985**	**0.9967**	**1,657.8**	**1,667.0**

[1]Two sided p-value

The fitted distribution parameters for the POT analysis presented in Table 14 indicate that the 2015 flood event increased the scale parameter by approximately 15 cms. Such increases led to a larger variance in the predicted runoff and increased the non-linearity of the quantile function for which design discharges can be estimated. The K-S test of the PP model produced a more significant influence from the event. This result is observed with the increase in the location parameter from approximately 411 cms to approximately 427 cms. Although the location parameter is a vital distribution parameter, the shape and scale parameters play a more influential role in the runoff estimation for the infrastructure design setting.

Table 14. Saluda River POT distribution parameters.

	Without 2015 Flood Event		With 2015 Flood Event	
Parameter	GP	**PP**	GP	**PP**
Location[1]	198.22	**411.40**	198.22	**427.54**
Scale[2]	118.32	**130.28**	119.98	**145.17**
Shape	0.05582	**0.05626**	0.10935	**0.10975**

[1]Threshold for the GP model
[2]Modified scale for the GP model

The GP and PP models presented in Figures 7a and 7b were used to construct return level predictions for the Saluda River. This result is presented in Figure 8. Like the two previous applications, the model return level function of each model appropriately represented the estimated discharge below the 10-year event, with more variation between the modeled and empirical results above the 10-year event.

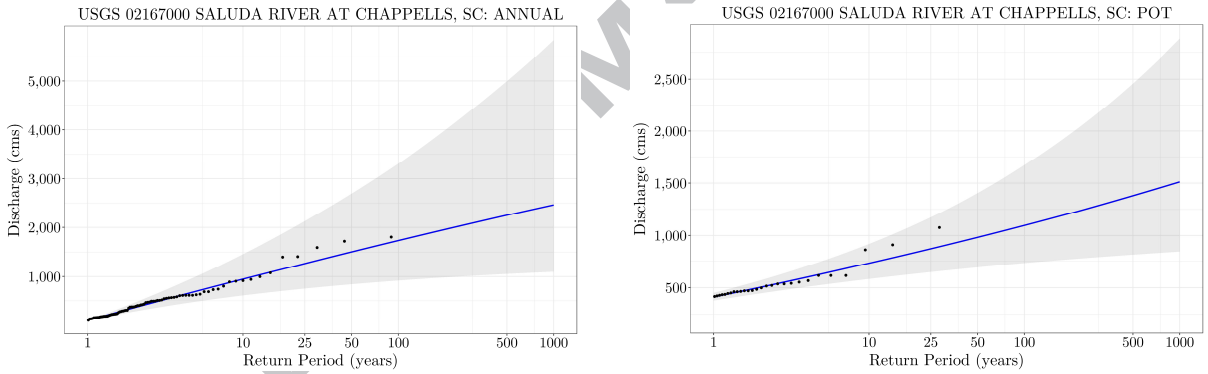

(a) **(b)**

Figure 8. Computed return levels for the Saluda River excluding the 2015 flood event for (a) AMF and (b) POT. Bootstrap 95% CIs are shown as the shaded region.

The BM approach predicted higher return level estimates when compared to the POT approach, although both followed the empirical data well and have comparable shape parameters. Further, reduced confidence intervals were generated from the POT model versus the AMF model. For example, the 100-year storm CI for the AMF model would be approximately 900 to 3,200 cms, while the POT CI would be

approximately 700 to 1,700 cms. Hence, for a common design storm such as the 100-year event, the AMF model has approximately 1,300 cms more variation in the predicted design discharge. On the other hand, the 100-year design discharge for the AMF model would be approximately 1,700 cms, while the POT model would be 1,100 cms, thereby representing a difference in the design discharges by approximately half the difference in the discharge variation. In this case, the AMF model has more than four times the available data of that compared to the POT model, making the selection of the AMF model much more appealing to infrastructure safety and reliability as opposed to the POT model.

The return period framework was extended to estimate the intensity of the 2015 event to be approximately 11.2 years and 51.7 years for the AMF and POT model, respectively. This result further exemplifies the uncertainty in design level estimates for this basin using the POT techniques presented herein when compared to the AMF model. For example, the AMF analysis resulted in a slightly negative shape parameter which did not experience a significant change with the inclusion of the 2015 event. However, the POT model experienced a positive shape parameter which doubled during the post-event analysis, hence increasing the non-linearity in the return level estimation. In this context, the AMF model showed less influence and severity due to the hurricane event when compared to the POT model, although with a much larger sampling size.

4.4. Analysis of the Congaree River

The Congaree River is located at the heart of Columbia, SC and drains more than 20,331 sqkm. Block maxima (i.e., 1982-2015) and POT (i.e., 10/01/1984-09/30/2015) datasets were developed from historical USGS datasets and used to construct probabilistic models of extreme flood events. Figure 10 reveals the results for the GEV, GP, Gumbel, and PP models through constructed CDF and probability plots without the 2015 event. The AMF results show that each model performed well when comparing the modeled probability to the empirical probabilities, of which the GEV appeared to be the best fit. The GEV and Gumbel models produced comparable distributions (i.e., CDFs), but a review of the Q-Q plots show much

more variability in the upper tail behavior of the Gumbel model (i.e., 5,000 cms to 10,000 cms). The GP and PP models provided satisfactory results below 10,000 cms for the distribution and quantile predictions, but well overpredicted the major flood event by more than 10,000 cms.

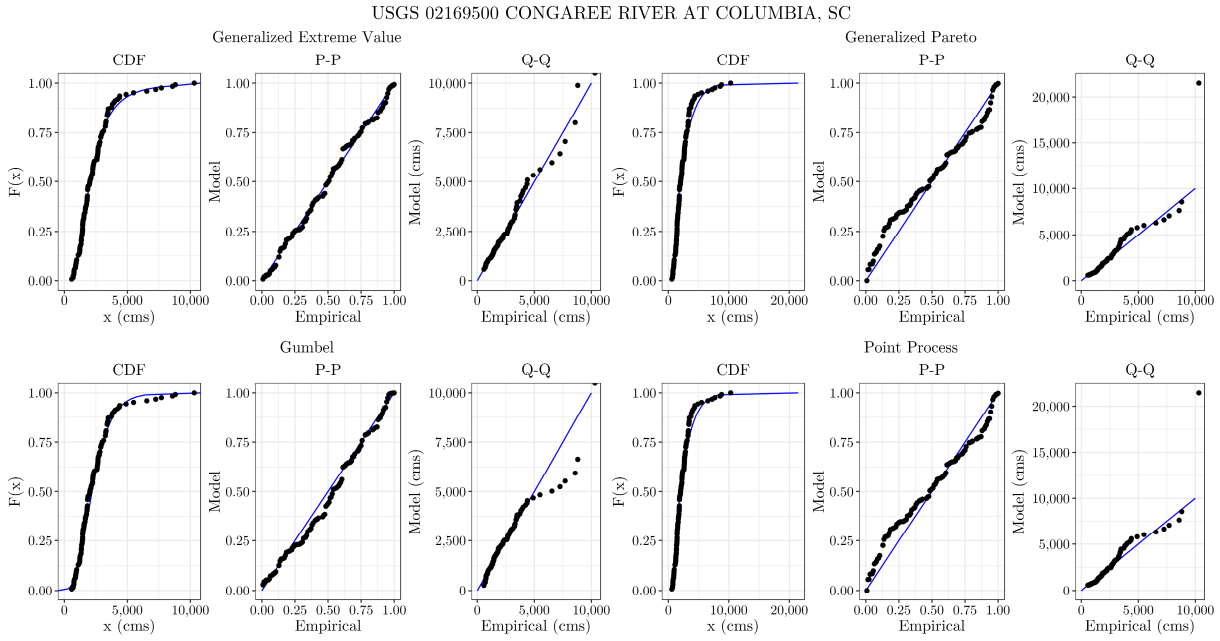

(a)

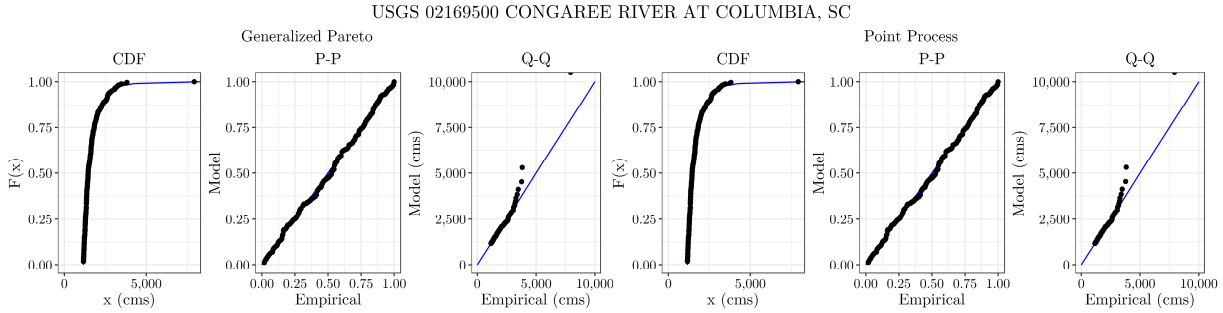

(b)

Figure 9. Congaree River diagnostic plots: (a) AMF series and (b) POT series.

It is evident that the observed patterns (i.e., for the mean and standard deviation) in the different quantile plots are not in the middle of the simulated bundle of curves but are compatible with the range of extreme

fluctuations and persistent. However, the quantile estimation method, like any statistical method, can be affected by the sampling uncertainty. The AMF performance summary outlined in Table 15 indicates that the GEV model was appropriately considered the parent distribution for the Congaree River flood data that represented the upper tail behavior of the empirical distribution quite well when compared to the rest of models.

Table 15. Congaree River AMF performance summary.

Without 2015 Flood Event							
Model	K-S[1]	C-vM[1]	A-D[1]	Pearson (ρ)	R^2	AIC	BIC
GEV	**0.7153**	**0.8769**	**0.8954**	**0.9976**	**0.9949**	**2,111.4**	**2,119.8**
GP	0.0284	0.0514	0.0309	0.9922	0.9582	2,122.3	2,127.9
GUMBEL	0.2534	0.4110	0.2870	0.9950	0.9830	2,124.6	2,130.2
PP	0.0283	0.0513	0.0309	0.9922	0.9581	2,372.3	2,380.8
With 2015 Flood Event							
Model	K-S[1]	C-vM[1]	A-D[1]	Pearson (ρ)	R^2	AIC	BIC
GEV	**0.7243**	**0.8907**	**0.9207**	**0.9977**	**0.9952**	**2,132.0**	**2,140.5**
GP	0.0323	0.0595	0.0369	0.9927	0.9607	2,142.1	2,147.8
GUMBEL	0.2363	0.3922	0.2824	0.9948	0.9825	2,145.2	2,150.9
PP	0.0322	0.0594	0.0369	0.9927	0.9607	2,394.1	2,402.6

[1]Two sided p-value.

The upper tail behavior of the GP and PP models demonstrated in the AMF diagnostic plots likely indicate the inadequacy of these models in approximating the block maxima time series for the Congaree River basin. Although, the length of AMF for the Congaree River is more than 120 years, the behavior of the extreme flood data did not follow Fréchet law as observed at the Saluda River basin.

Inclusion of the 2015 flood event within the AMF analysis (i.e., AMF-2015) had the least amount of effect on the performance of the probability models compared to the three previous applications. In this case, the Congaree River basin is the largest of the four study areas, thus exhibiting larger runoff lag times

and response levels for the same meteorological setting. The longer time series and larger basin size is expected to enable the flood distribution to be less affected by additional extreme events.

No significant (i.e., < 0.05) changes were observed in the AMF shape parameter estimates with the inclusion of the 2015 flood event (Table 16), thus suggesting the event does not appear to affect the distribution or cause a larger degree of uncertainty in the model fitting. The GEV served as the most appropriate AMF distribution with a minimal increase in the estimated shape parameter by 0.003. Conversely, the scale parameter experienced an increase of approximately 11 cms. In this case, the 2015 flood is indicated to be a larger event (increase in location parameter) and introduces more variability in runoff deviation, nonetheless the runoff rate for any given return level is nearly constant.

Table 16. Congaree River AMF distribution parameters.

	Without 2015 Food Event				**With 2015 Flood Event**			
Parameter	**GEV**	GP	GUMBEL	PP	**GEV**	GP	GUMBEL	PP
Location[1]	**1,703.97**	580.47	1,834.89	580.51	**1,713.82**	580.47	1,847.94	580.50
Scale[2]	**868.58**	2,082.71	998.17	2,082.17	**879.67**	2,117.50	1,012.66	2,117.07
Shape	**0.2531**	-0.0996	-	-0.0997	**0.2569**	-0.1053	-	-0.1054

[1]Threshold for the GP model
[2]Modified scale for the GP model

The performance summary for the Congaree POT time series excluding the 2015 flood provided in Table 17 shows a strong consideration for the GP or PP as a parent distribution when considering the significance level of the cumulative frequency distribution. However, Bayesian criterion suggests that the PP model should be selected. In this case, the traditional hypothesis tests produced nearly identical results, but a fair comparison of the information based criteria (i.e., BIC/AIC) quickly differentiates the underlying distribution.

Table 17. Congaree River POT performance summary.

Without 2015 Flood Event							
Model	K-S[1]	C-vM[1]	A-D[1]	Pearson (ρ)	R^2	AIC	BIC
GP	0.9358	0.9113	0.9317	0.9991	0.9979	3,829.3	3,836.4
PP	**0.9325**	**0.9102**	**0.9320**	**0.9990**	**0.9979**	**3,218.7**	**3,229.5**
With 2015 Flood Event							
Model	K-S[1]	C-vM[1]	A-D[1]	Pearson (ρ)	R^2	AIC	BIC
GP	0.9564	0.9141	0.9388	0.9991	0.9980	3,888.9	3,896.0
PP	**0.9554**	**0.9146**	**0.9389**	**0.9991**	**0.9980**	**3,265.8**	**3,276.5**

[1]Two sided p-value

Extension of the POT time series to include the entirety of the 2015 flood event did not significantly affect the PP model. For example, the PP scale and shape parameters prior to the 2015 event were 636.62 cms and 0.1810, respectively, while the influence of the 2015 flood increased the scale and shape to 677.86 cms and 0.2085, correspondingly (see Table 18). While the shape parameter is only marginally affected, the scale parameter does experience an increase by more than 6.5%. An important result demonstrated in Table 17 is the fact that the performance of each model slightly improved with the inclusion of the 2015 flood event data, thus there is ultimately a degree of influence.

Table 18. Congaree River POT distribution parameters.

	Without 2015 Food Event		**With 2015 Flood Event**	
Parameter	GP	**PP**	GP	**PP**
Location[1]	1,160.99	**2,299.16**	1,160.99	**2,344.43**
Scale[2]	430.47	**636.62**	431.32	**677.86**
Shape	0.17990	**0.1810**	0.2083	**0.2085**

[1]Threshold for the GP model
[2]Modified scale for the GP model

Figure 10 shows the predicted return levels with bootstrapped 95% CIs assuming the GEV and PP models as parent distributions for the AMF and POT analyses, respectively. In this case, the AMF frequency analysis resulted in a return period function which more adequately mimicked the empirical behavior of

the underlying distribution when compared to the POT frequency analysis. It is important to note that the PP parameterization used herein is given in terms of the GEV block maxima parameters and then further re-parameterized as a threshold model in terms of the GP derivation.

Both the AMF and POT return level functions had comparable underlying function shapes (i.e., AMF = 0.25 vs. POT = 0.18), as with the Enoree River and the Saluda River applications, while the underlying scale of the AMF model was much higher (i.e., AMF = 868.6 cms vs. POT = 636.6 cms). For example, the estimated 100-year runoff for the AMF model was just below 10,000 cms, while the POT model estimated slightly less than 7,500 cms (Figure 10). In this case, the design level discharge is approximately 2,500 cms less for the POT approach. This result is like that of the Saluda River application in that the AMF model produces consistently higher design discharges but based on more than 100 years of historical data as opposed to the POT model which is based on approximately 35 years of historical records. As stated in the analysis of other applications, the small size of the samples tend to hide the true distribution and the heavy tail fluctuation.

A peak flow rate of 5,239 cms registered for the Congaree River during hurricane Joaquin. The models presented herein (i.e., GEV and PP) estimated a return period of 16.9 years and 29.2 years for the AMF and POT series, respectively. The intense rainfall which was categorized as a 1,000-year storm did not directly correlate to such an extreme event for the direct runoff (i.e., river discharge) within the Congaree basin. However, extensive hydraulics structures (e.g., dams, ponds, levees, etc.) in the study region can delay and mitigate peak runoff and substantially affect distribution family.

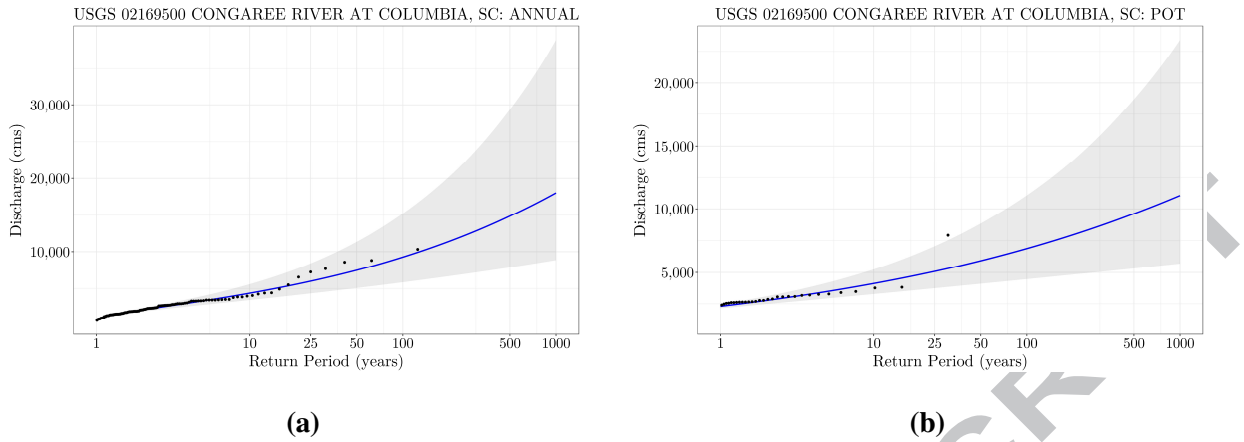

(a) **(b)**

Figure 10. Computed return levels for the Congaree River excluding the 2015 flood event for (a) AMF and (b) POT. Bootstrap 95% confidence intervals are shown as the shaded region.

5. Conclusions

This paper provided a critical analysis of stochastic flood frequency analysis using four real-world applications from North Carolina and South Carolina, USA. The aim was to explore the inferences involved in extreme modeling, the available methods/tools, and explicitly highlight the modeling difficulties and the role of uncertainty in flood frequency analysis. Two types of time series were evaluated, the first method employed historical annual maximum flood data, AMF, collected by USGS, while the second incorporated daily maximum flood data or POT. The AMF incorporated all annual data points, while the POT series incorporated all daily maximum data above a specific threshold defined based on statistical goodness of fit tests. Four extreme value probability distributions were selected and tested based on statistical fitting: i) Generalized Extreme Value; ii) Generalized Pareto; iii) Gumbel; and iv) Point Process. Of these methods, the GP and PP models are parameterized in terms of threshold exceedances for the POT dataset.

Evaluation of the extreme events was first based on statistical testing of the data with and without the inclusion of the 2015 flood event that occurred in the Carolinas. The results indicated that the 2015 flood event does affect some of the probability distributions but does not appear to cause statistically significant

influences on the selected parent distribution. Focusing on the geographical distribution of the fitted distributions in the study region, the analyses suggest that large urban and rural areas share approximately the same distributions (i.e., GEV), whereas less developed areas exhibit light- to heavy-tailed behaviors (i.e., Gumbel and GP). The AMF analysis of Rocky Creek favors the use of the Gumbel distribution and does not provide any evidence of its outperformance over the Fréchet law. Saluda River, on the other hand, showed the best fit to GP with a negative shape parameter. Here, we would suggest that this should not be used in the case where flood data propose an extreme distribution with a negative shape parameter. Instead, it makes more sense and seems more reasonable to use a Gumbel distribution as recommended by Papalexiou and Koutsoyiannis, 2013. In addition, the analysis of the estimated GEV shape parameters of the AMF data for the Enoree and Congaree basins revealed a close relationship between these two basins and suggests that the distribution of the GEV shape parameter, that would emerge if extremely large samples were available, is slightly shifted toward a heavier-tail when the October 2015 flood was included (≈ 0.25). However, as stated by Papalexiou and Koutsoyiannis, 2013, only very large samples can reveal the true distribution of the shape parameter and actual variability of the underlying process.

Further, modeling results of the POT series showed the best fit with the PP distribution for four applications. In all cases, the average value of the PP shape parameter increased and tended to a positive value as the October 2015 POT values were included to the time series (i.e., the record length increased). Under the hypothesis of the existence of an asymptotic distribution for the shape parameter, it has been demonstrated that the apparent exponential decay of the upper tail of the POT distribution observed in short time series is coherent with an asymptotic process which fluctuates around an average heavy tail behavior and affects return level estimation and its uncertainty.

Dealing with extreme analysis, uncertainty affects not only the distribution model, but also the exploratory diagnostics. This study used the nonparametric and parametric bootstrap method or Monte Carlo simulation model to compute CIs of distribution models and the estimators. The empirical

distribution of the bootstrap method showed a close relationship with the actual distribution (i.e., asymptotic assumptions) and easily met specific requirements of the four applications. Therefore, we suggest the bootstrap method as a practical approach to obtain CIs, however more advanced methods such as Bayesian approaches can be applied to reduce the uncertainty by incorporating exogenous information (i.e., a variable originates externally, but has influences within a drainage system).

Based on these analyses, the answer for the research question of "how extreme was the October 2015 flood in the Carolinas?" raised earlier is that there is insufficient evidence to show that the 2015 flood event affected the parent distribution model of the annual series, but certainty affected the POT series in terms of shifting the shape parameter towards a heavier tail. However, tail fluctuations that are caused by i) mixture of extreme observational data and their thresholds and ii) temporal fluctuations of the parent distribution and/or its parameters over long time scales may introduce significant uncertainty and make extreme inference difficult. While this research tends to diminish the impact of the first fluctuation by analysis of different applications, time series, and thresholds, the latter one is correlated with the fluctuation of physical mechanisms driving the runoff process, such as dam construction, land use changes/site development, etc., as recently advocated by Samadi and Meadows, 2017.

Further research is required to understand the true behavior of runoff in the study region. For instance, the inclusion of independent variables (e.g., reservoir factor) can be employed as covariates to check for monotonic trends, abrupt changes, or more complex nonlinear temporal patterns and relationships between flood dynamics and watershed factors. In this context, possible deterministic predictable mechanisms can be applied to identify (temporal/permanent) evolution of drainage systems. If necessary, such an assessment should be complemented by other criteria, such as risk of failure in the design life and cost benefit analyses/considerations, by accounting for the different sources of uncertainty (e.g., distribution parameters, quantile estimates, and sampling uncertainty).

Finally, this research provides a consistent and practical procedure to model floods which can be applied to other hydrological extremes (e.g., rainfall). The key implication of this analysis is that increasing the magnitude and frequency of runoff particularly for peak over threshold events is more probable at least for the four applications presented here, thus the classical frequency analysis may underestimate the flood magnitude. This result is seen in the context of the Saluda and Congaree basins, which experience major changes in the estimated shape parameters for the POT analysis and should not be blindly assumed to occur elsewhere. However, a similar analysis could be thoroughly applied to study regions around the globe to grasp a greater understanding of changing flood distributional behavior in response to extreme events and aid in advancing resilient infrastructure design. Engineering design and practice need to move from simple methods to more practical/advanced approaches that acknowledge the shifting of extremes from exponential law toward heavier tailed probability distributions.

6. Acknowledgments

This research was supported by SC Sea Grant Consortium (Grant # 15520-GA11) and the University of South Carolina (grant # 15520-16-40787 and 15520-17-44716). The analyses were performed using the "ismev" and "extRemes" packages in R (R Development Core Team, 2013). The authors and maintainers of these tools are gratefully acknowledged.

7. References

Balkema, A.A., de Haan, L., 1974. Residual life time at great age. Ann. Probab. 792–804.

Bernardara, P., Schertzer, D., Sauquet, E., Tchiguirinskaia, I., Lang, M., 2008. The flood probability distribution tail: how heavy is it? Stoch. Environ. Res. Risk Assess. 22, 107–122.

Chen, X., Shao, Q., Xu, C.-Y., Zhang, J., Zhang, L., Ye, C., 2017. Comparative Study on the Selection Criteria for Fitting Flood Frequency Distribution Models with Emphasis on Upper-Tail Behavior. Water 9, 320.

Coles, S., 2001. An introduction to statistical modeling of extreme values. Springer.

Cooley, D., 2013. Return Periods and Return Levels Under Climate Change. Springer Netherlands, Dordrecht, pp. 97–114.

Davison, A.C., Smith, R.L., 1990. Models for exceedances over high thresholds. J. R. Stat. Soc. Ser. B 393–442.

Di Baldassarre, G., Laio, F., Montanari, A., 2009. Design flood estimation using model selection criteria. Phys. Chem. Earth, Parts A/B/C 34, 606–611.

Efron, B., Tibshirani, R.J., 1993. An Introduction to the Bootstrap: Monographs on Statistics and Applied Probability, Vol. 57. New York London Chapman Hall/CRC.

El Adlouni, S., Bobée, B., Ouarda, T., 2008. On the tails of extreme event distributions in hydrology. J. Hydrol. 355, 16–33.

Fisher, R.A., Tippett, L.H.C., 1928. Limiting forms of the frequency distribution of the largest or smallest member of a sample, in: Mathematical Proceedings of the Cambridge Philosophical Society. pp. 180–190.

Fuller, W.E., 1914. Flood flows. Trans. Am. Soc. Civ. Eng. 77, 564–617.

Gnedenko, B., 1943. Sur la distribution limite du terme maximum d'une serie aleatoire. Ann. Math. 423–453.

Goda, Y., 2011. Plotting-position estimator for the L-moment method and quantile confidence interval for the GEV, GPA, and Weibull distributions applied for extreme wave analysis. Coast. Eng. J. 53, 111–149.

Gubareva, T.S., Gartsman, B.I., 2010. Estimating distribution parameters of extreme hydrometeorological characteristics by L-moments method. Water Resour. 37, 437–445.

Gumbel, E.J., 1958. Statistics of extremes. 1958. Columbia Univ. Press. New York.

Hosking, J.R.M., Wallis, J.R., Wood, E.F., 1985. Estimation of the generalized extreme-value distribution by the method of probability-weighted moments. Technometrics 27, 251–261.

Jenkinson, A.F., 1955. The frequency distribution of the annual maximum (or minimum) values of meteorological elements. Q. J. R. Meteorol. Soc. 81, 158–171.

Kottegoda, N.T., Rosso, R., 2008. Applied Statistics for Civil and Environmental Engineers. Blackwell Malden, MA.

Koutsoyiannis, D., 2005. Uncertainty, entropy, scaling and hydrological stochastics. 1. Marginal distributional properties of hydrological processes and state scaling / Incertitude, entropie, effet d'échelle et propriétés stochastiques hydrologiques. 1. Propriétés distributionnel. Hydrol. Sci. J. 50. https://doi.org/10.1623/hysj.50.3.381.65031

Koutsoyiannis, D., 2004. Statistics of extremes and estimation of extreme rainfall: I. Theoretical investigation/Statistiques de valeurs extrêmes et estimation de précipitations extrêmes: I. Recherche théorique. Hydrol. Sci. J. 49.

Laio, F., Di Baldassarre, G., Montanari, A., 2009. Model selection techniques for the frequency analysis of hydrological extremes. Water Resour. Res. 45.

Leadbetter, M.R., Lindgren, G., Rootzen, H., 1983. Extremes and Related Properties of Random Sequences and Series.

Maidment, D.R., 1993. Handbook of Hydrology. McGraw-Hill New York.

Martinkova, M., 2013. A review of applied methods in Europe for flood-frequency analysis in a changing environment:Floodfreq COST action ES0901: European procedures for flood frequency estimation. Centre for Ecology & Hydrology on behalf of COST.

Martins, E.S., Stedinger, J.R., 2000. Generalized maximum-likelihood generalized extreme-value quantile estimators for hydrologic data. Water Resour. Res. 36, 737–744.

Martins, E.S., Stedinger, J.R., 2001. Generalized Maximum Likelihood Pareto-Poisson estimators for partial duration series. Water Resour. Res. 37, 2551–2557.

McMahon, T.A., Vogel, R.M., Peel, M.C., Pegram, G.G.S., 2007. Global streamflows--Part 1: Characteristics of annual streamflows. J. Hydrol. 347, 243–259.

Michele, C. De, Rosso, R., 2001. Uncertainty Assessment of Regionalized Flood Frequency Estimates. J. Hydrol. Eng. 6, 453–459.

Mohssen, M.A.W., 2009. Partial duration series in the annual domain.

Mondal, A., Mujumdar, P.P., 2015. Return levels of hydrologic droughts under climate change. Adv. Water Resour. 75, 67–79.

Obeysekera, J., Salas, J.D., 2014. Quantifying the Uncertainty of Design Floods under Nonstationary Conditions. J. Hydrol. Eng. 19, 1438–1446.

Papalexiou, S.M., Koutsoyiannis, D., Makropoulos, C., 2013. How extreme is extreme? An assessment of daily rainfall distribution tails. Hydrol. Earth Syst. Sci. 17, 851–862.

Papalexiou, S.M., Koutsoyiannis, D., 2013. Battle of extreme value distributions: A global survey on extreme daily rainfall. Water Resour. Res. 49, 187–201.

Pickands III, J., 1975. Statistical inference using extreme order statistics. Ann. Stat. 119–131.

Pourreza-Bilondi, M., Samadi, S.Z., Akhoond-Ali, A.-M., Ghahraman, B., 2017. Reliability of Semiarid Flash Flood Modeling Using Bayesian Framework. J. Hydrol. Eng. 22, 5016039.

R Core Team, 2013. R: A Language and Environment for Statistical Computing.

Renard, B., Sun, X., Lang, M., 2013. Bayesian Methods for Non-stationary Extreme Value Analysis, in: Extremes in a Changing Climate: Detection, Analysis and Uncertainty. Springer Netherlands, Dordrecht, pp. 39–95.

Resnick, S.I., 1987. Extreme values, regular variation, and point processes. Springer-Verlag, New York.

Rootzén, H., Katz, R.W., 2013. Design life level: quantifying risk in a changing climate. Water Resour. Res. 49, 5964–5972.

Saeed Far, S., Abd. Wahab, A.K., 2016. Evaluation of Peaks-Over-Threshold Method. Ocean Sci. Discuss. 2016, 1–25.

Samadi, S.Z., Meadows, M.E., 2017. The Transferability of Terrestrial Water Balance Components under Uncertainty and Nonstationarity: A Case Study of the Coastal Plain Watershed in the Southeastern USA. River Res. Appl. 33, 796–808.

Samadi, S., Wilson, C.A.M.E., Moradkhani, H., 2013. Uncertainty analysis of statistical downscaling models using Hadley Centre Coupled Model. Theor. Appl. Climatol. 114, 673–690.

Serinaldi, F., Kilsby, C.G., 2014. Rainfall extremes: Toward reconciliation after the battle of distributions. Water Resour. Res. 50, 336–352.

Serinaldi, F., Kilsby, C.G., 2015. Stationarity is undead: Uncertainty dominates the distribution of extremes. Adv. Water Resour. 77, 17–36.

Smith, R.L., 1989. Extreme value analysis of environmental time series: An application to trend detection in ground-level ozone. Stat. Sci. 367–377.

Stedinger, J.R., Griffis, V.W., 2011. Getting from here to where? Flood frequency analysis and climate. JAWRA J. Am. Water Resour. Assoc. 47, 506–513.

Villarini, G., Smith, J.A., Ntelekos, A.A., Schwarz, U., 2011. Annual maximum and peaks-over-threshold analyses of daily rainfall accumulations for Austria. J. Geophys. Res. Atmos. 116.

Vogel, R.M., Wilson, I., 1996. Probability Distribution of Annual Maximum, Mean, and Minimum Streamflows in the United States. J. Hydrol. Eng. 1, 69–76.

Vogel, R.M., Yaindl, C., Walter, M., 2011. Nonstationarity: Flood magnification and recurrence reduction factors in the United States. JAWRA J. Am. Water Resour. Assoc. 47, 464–474.

von Mises, R., 1936. La Distribution de la Plus Grande de n Valeurs, Vol. 2 of Selected Papers of Richard von Mises. Provid. RI Am. Math. Soc. 294.

- The October 2015 flooding in the Carolinas is analyzed using various distributions
- GEV/GP were recommended as the parent distributions for the Carolinas annual flood
- Monte Carlo model provided a realistic asymmetric confidence interval
- Engineering design should move from simple methods to more practical approaches